Electronic Supplementary Material (ESI) for Materials Advances.

Halogen Substituted Tetraphenylethylene AIEgens: Facile Single-Crystal-to-Single-Crystal Transformation, Polymorphism and Mechanofluorochromism

Yong Cao[a], Chengjun Pan*[a][b]and Jinjia Xu*[b]

[a] Shenzhen Key Laboratory of Polymer Science and Technology, College of Materials Science and Engineering, Shenzhen University, Shenzhen 518060, China.

E-mail: pancj@szu.edu.cn

[b] Department of Chemistry and Biochemistry, University of Missouri-St. Louis, MO, 63121, United States.

Email: jxbgk@umsystem.edu

Table of contents:

1. Synthesis of the compounds

All available reagents and solvents were used as received without further purification. 4-(1,2,2-triphenylvinyl)benzaldehyde was purchased from Alfa Aesar. 2-(4-fluorophenyl)acetonitrile, 2-(4-chlorophenyl)acetonitrile, 2-(4-bromophenyl)acetonitrile, 2-(4-iodophenyl)acetonitrile, 2-(3-fluorophenyl)acetonitrile, 2-(3-chlorophenyl)acetonitrile, 2-(3-bromophenyl)acetonitrile, 2-(3-iodophenyl)acetonitrile, sodium methoxide and the solvents (HPLC grade) for crystallization were purchased from Energy Chemical.

1.1. General procedure for the preparation of TPE derivatives

The TPE derivatives were prepared according to the previously reported procedure .[1] The respective phenylacetonitrile (1.2 equivalents) and sodium methoxide (2 equivalents) were added to a stirred solution of 4-(1,2,2-triphenylvinyl)benzaldehyde (0.5 g, 1.0 equivalent) in methanol. The mixture was stirred at room temperature for 24 h and then the products precipitated out. After that, the yellow precipitate was filtered out and washed with cold methanol, and then dried in a vacuum.

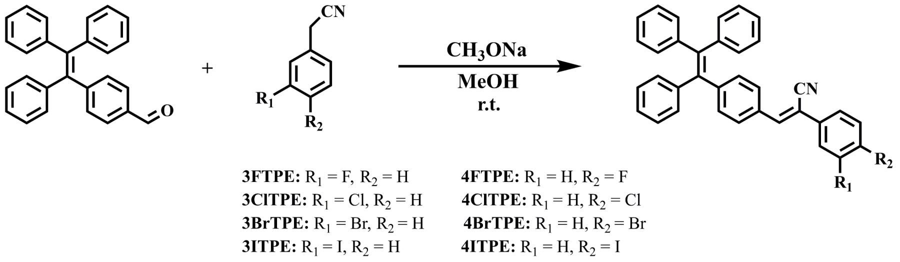

3FTPE: R_1 = F, R_2 = H
3ClTPE: R_1 = Cl, R_2 = H
3BrTPE: R_1 = Br, R_2 = H
3ITPE: R_1 = I, R_2 = H
4FTPE: R_1 = H, R_2 = F
4ClTPE: R_1 = H, R_2 = Cl
4BrTPE: R_1 = H, R_2 = Br
4ITPE: R_1 = H, R_2 = I

Scheme S1. Synthesis of the **TPE** derivatives.

1.1.1. 2-(4-fluorophenyl)-3-(4-(1,2,2-triphenylvinyl)phenyl)acrylonitrile (4FTPE)

Bright yellow colored solid. Yield: (88%). ^{1}H NMR (500 MHz, $CDCl_3$, TMS, RT): δ/ppm 7.64 (d, J = 8.3 Hz, 2H), 7.60 (ddd, J = 8.2, 5.2, 2.6 Hz, 2H), 7.33 (s, 1H), 7.16 – 7.09 (m, 13H), 7.08 – 7.01 (m, 6H). ^{13}C NMR (126 MHz, $CDCl_3$, TMS, RT): δ/ppm 164.07, 162.08, 146.56, 143.28, 143.25, 143.12, 142.36, 141.81, 141.80, 139.94, 131.91, 131.42, 131.32, 131.28, 131.24, 130.88, 130.86, 128.66, 127.87, 127.82, 127.76, 127.69, 127.65, 126.87, 126.70, 126.68, 118.00, 116.17, 115.99, 109.50. MALDI-TOF-MS (m/z): [M+H]$^+$ calcd for $C_{35}H_{24}FN$, 478.189; found 478.097.

1.1.2. 2-(4-chlorophenyl)-3-(4-(1,2,2-triphenylvinyl)phenyl)acrylonitrile (4ClTPE)

Pale yellow colored solid. Yield: (90%). ^{1}H NMR (500 MHz, $CDCl_3$, TMS, RT): δ/ppm 7.65 (d, J = 8.3 Hz, 2H), 7.56 (d, J = 8.7 Hz, 2H), 7.39 (d, J = 8.7 Hz, 2H), 7.38 (s, 1H), 7.15 – 7.09 (m, 11H), 7.07 – 7.01 (m, 6H). ^{13}C NMR (126 MHz, $CDCl_3$, TMS, RT): δ/ppm 146.92, 143.41, 143.38, 143.25, 142.56, 142.33, 140.06, 135.18, 133.34, 132.09, 131.47, 131.43, 131.39, 129.37, 128.93, 128.03, 127.99, 127.81, 127.25, 127.05, 126.87, 126.85, 117.96, 109.54. MALDI-TOF-MS (m/z): [M+H]$^+$ calcd for $C_{35}H_{24}ClN$, 494.160; found 494.084.

1.1.3. 2-(4-bromophenyl)-3-(4-(1,2,2-triphenylvinyl)phenyl)acrylonitrile (4BrTPE)

Pale yellow colored solid. Yield: (92%). ^{1}H NMR (500 MHz, $CDCl_3$, TMS, RT): δ/ppm 7.65 (d, J = 8.3 Hz, 2H), 7.55 (d, J = 8.8 Hz, 2H), 7.49 (d, J = 8.8 Hz, 2H), 7.39 (s, 1H), 7.15 – 7.09 (m, 11H), 7.07 – 7.01 (m, 6H). ^{13}C NMR (126 MHz, $CDCl_3$, TMS, RT): δ/ppm 146.97, 143.42, 143.39, 143.25, 142.61, 142.38, 140.07, 133.82, 132.34, 132.11, 131.48, 131.46, 131.44, 131.40, 128.96, 128.04, 128.00, 127.82, 127.51, 127.06, 126.89, 126.86, 123.36, 117.91, 109.60. MALDI-TOF-MS (m/z): $[M+H]^+$ calcd for $C_{35}H_{24}BrN$, 538.109; found 538.172.

1.1.4. 2-(4-iodophenyl)-3-(4-(1,2,2-triphenylvinyl)phenyl)acrylonitrile (4ITPE)

Pale yellow colored solid. Yield: (95%). ^{1}H NMR (500 MHz, $CDCl_3$, TMS, RT): δ/ppm 7.75 (d, J = 8.6 Hz, 2H), 7.65 (d, J = 8.4 Hz, 2H), 7.40 (s, 1H), 7.36 (d, J = 8.6 Hz, 2H), 7.15 – 7.09 (m, 11H), 7.07 – 7.00 (m, 6H). ^{13}C NMR (126 MHz, $CDCl_3$, TMS, RT): δ/ppm 146.89, 143.32, 143.28, 143.14, 142.51, 142.25, 139.97, 138.18, 134.33, 132.01, 131.38, 131.34, 131.30, 128.88, 127.94, 127.90, 127.72, 127.52, 126.96, 126.78, 126.76, 117.75, 109.61, 94.88. MALDI-TOF-MS (m/z): $[M+H]^+$ calcd for $C_{35}H_{24}IN$, 586.095; found 586.134.

1.1.5. 2-(3-fluorophenyl)-3-(4-(1,2,2-triphenylvinyl)phenyl)acrylonitrile (3FTPE)

Bright yellow colored solid. Yield: (90%). ^{1}H NMR (500 MHz, $CDCl_3$, TMS, RT): δ/ppm 7.66 (d, J = 8.3 Hz, 2H), 7.44 – 7.36 (m, 3H), 7.35 – 7.31 (m, 1H), 7.16 – 7.09 (m, 11H), 7.09 – 7.01 (m, 7H). ^{13}C NMR (126 MHz, $CDCl_3$, TMS, RT): δ/ppm 164.14, 162.17, 147.01, 143.35, 143.31, 143.18, 142.92, 142.58, 139.99, 137.01, 136.95, 132.05, 131.42, 131.38, 131.34, 131.27, 130.72, 130.66, 128.98, 127.99, 127.94, 127.76, 127.01, 126.83, 126.80, 121.77, 121.74, 117.85, 116.11, 115.94, 113.00, 112.81, 109.50, 109.47. MALDI-TOF-MS (m/z): $[M+H]^+$ calcd for $C_{35}H_{24}FN$, 478.189; found 478.078.

1.1.6. 2-(3-chlorophenyl)-3-(4-(1,2,2-triphenylvinyl)phenyl)acrylonitrile (3ClTPE)

Pale yellow colored solid. Yield: (92%). ^{1}H NMR (500 MHz, $CDCl_3$, TMS, RT): δ/ppm 7.66 (d, J = 8.4 Hz, 2H), 7.61 (s, 1H), 7.52 (dt, J = 6.9, 2.0 Hz, 1H), 7.40 (s, 1H), 7.38 – 7.33 (m, 2H), 7.12 (tt, J = 6.5, 3.6 Hz, 11H), 7.08 – 7.00 (m, 6H). ^{13}C NMR (126 MHz, $CDCl_3$, TMS, RT): δ/ppm 147.11, 143.40, 143.36, 143.23, 143.10, 142.65, 140.04, 136.65, 135.27, 132.11, 131.47, 131.43, 131.40, 131.32, 130.38, 129.16, 129.04, 128.04, 128.00, 127.81, 127.07, 126.88, 126.86, 126.01, 124.28, 117.86, 109.32. MALDI-TOF-MS (m/z): $[M+H]^+$ calcd for $C_{35}H_{24}ClN$, 494.160; found 494.061.

1.1.7. 2-(3-bromophenyl)-3-(4-(1,2,2-triphenylvinyl)phenyl)acrylonitrile (3BrTPE)

Pale yellow colored solid. Yield: (94%).^{1}H NMR (500 MHz, $CDCl_3$, TMS, RT): δ/ppm 7.77 (t, J = 1.8 Hz, 1H), 7.66 (d, J = 8.3 Hz, 2H), 7.58 – 7.55 (m, 1H), 7.51 – 7.48 (m, 1H), 7.40 (s, 1H), 7.30 (t, J = 7.9 Hz, 1H), 7.12 (tt, J = 6.5, 3.6 Hz, 11H), 7.08 – 7.01 (m, 6H). ^{13}C NMR (126 MHz, $CDCl_3$, TMS, RT): δ/ppm 146.95, 143.22, 143.18, 143.05, 142.97, 142.48, 139.86, 136.72, 131.93, 131.90, 131.30, 131.26, 131.22, 131.13, 130.44, 128.87, 128.70, 127.86, 127.82, 127.64, 126.90, 126.71, 126.68, 124.57, 123.16, 117.66, 109.01. MALDI-TOF-MS (m/z): $[M+H]^+$ calcd for $C_{35}H_{24}BrN$, 538.109; found 538.138.

1.1.8. 2-(3-iodophenyl)-3-(4-(1,2,2-triphenylvinyl)phenyl)acrylonitrile (3ITPE)

Pale yellow colored solid. Yield: (96%). ^{1}H NMR (500 MHz, $CDCl_3$, TMS, RT): δ/ppm 7.95 (t, J = 1.7 Hz, 1H), 7.71 – 7.68 (m, 1H), 7.65 (d, J = 8.3 Hz, 2H), 7.59 (ddd, J = 7.9, 1.8, 0.9 Hz, 1H), 7.38 (s, 1H), 7.18 – 7.09 (m, 12H), 7.08 – 7.01 (m, 6H). ^{13}C NMR (126 MHz, $CDCl_3$, TMS, RT): δ/ppm 147.05, 143.37, 143.32, 143.19, 143.05, 142.61, 140.01, 138.00, 136.91, 134.69, 132.06, 131.44, 131.39, 131.36, 131.30, 130.66, 129.00, 128.00, 127.96, 127.77, 127.03, 126.84, 126.82, 125.35, 117.76, 109.00, 94.89. MALDI-TOF-MS (m/z): $[M+H]^+$ calcd for $C_{35}H_{24}IN$, 586.095; found 585.782.

2. Preparation of the crystals

2.1. General procedure for the preparation of TPE derivative crystals

Preparation of crystals in methanol and acetonitrile: The crystallization in acetonitrile was accomplished by standing the acetonitrile solution of the compound at 8 °C for about 7 days (such solutions contained 20 mg of the compound in 5 mL of acetonitrile). The crystallization process of crystals in methanol was the same as that of crystals in acetonitrile, except that such solutions contained 10 mg of the compound in 5 mL of methanol (Figure S1a).

Preparation of crystals in DMF and DMSO: Similar to crystallization in acetonitrile and methanol, the crystallization in DMF or DMSO was completed by standing the DMF or DMSO solution of the compound at room temperature for about 7 days (such solutions contained 20 mg of the compound in 1 mL of DMF or DMSO). The difference was that the 3 mL sample bottle was used for crystallization here, and the 25 mL small beaker was used before (Figure S1b).

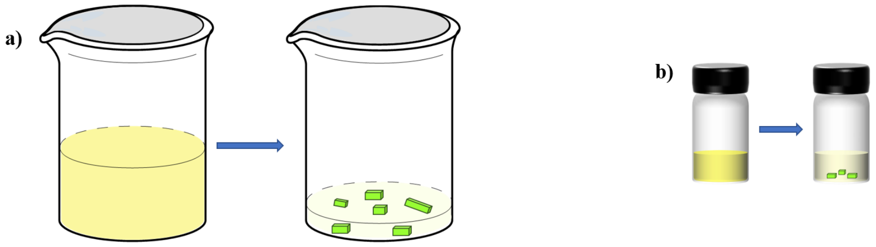

Figure S1. Schematic representation of the crystallization of the compound in methanol and acetonitrile (a), and the crystallization in DMF and DMSO (b).

2.2. General procedure for the preparation of thermally stimulated crystals

Thermally stimulated crystals were obtained by laying the corresponding crystals obtained in a solvent on a glass plate and then heating them on a heating table for a certain time (Figure S2). 4ClTPE (CH_3CN)(heated) crystal was obtained by heating 4ClTPE (CH_3CN) crystal at 60 °C for 30 minutes. 4BrTPE (CH_3CN)(heated) crystal was obtained by heating 4BrTPE (CH_3CN) crystal at 52 °C for 30 minutes. 3BrTPE (DMSO)(heated) crystal was obtained by heating 3BrTPE (DMSO) crystal at 88 °C for 30 minutes.

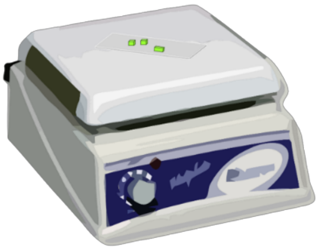

Figure S2. Schematic representation of the preparation of thermally stimulated crystals.

3. Characterization

NMR spectra were recorded on a Bruker Avance III 500 MHz spectrometer. Mass spectra of the compounds were measured on an Autoflex Matrix-Assisted Laser Desorption/Ionization Time of Flight (MALDI-TOF) mass spectrometer. The morphology of the crystals was observed with a Leica Dmi8 fluorescence microscope and Axio polarizing microscope. Fluorescence spectra were recorded using Thermoscientific. Fluorescence quantum yields of the solid samples were obtained on a Hamamatsu Absolute PL Quantum yield spectrometer. Differential scanning calorimetry (DSC) was carried out on a Hitachi thermal analyzer system (DSC7020). The Powder X-ray diffraction patterns were recorded using XRD-Rigaku with Cu $K\alpha$ radiation (λ = 1.540500 Å) operated in the 2θ range from 5° to 50°. Single crystal X-ray diffraction were performed on a Rigaku XtaLAB PRO diffractometers.

4. Polymorphism studies

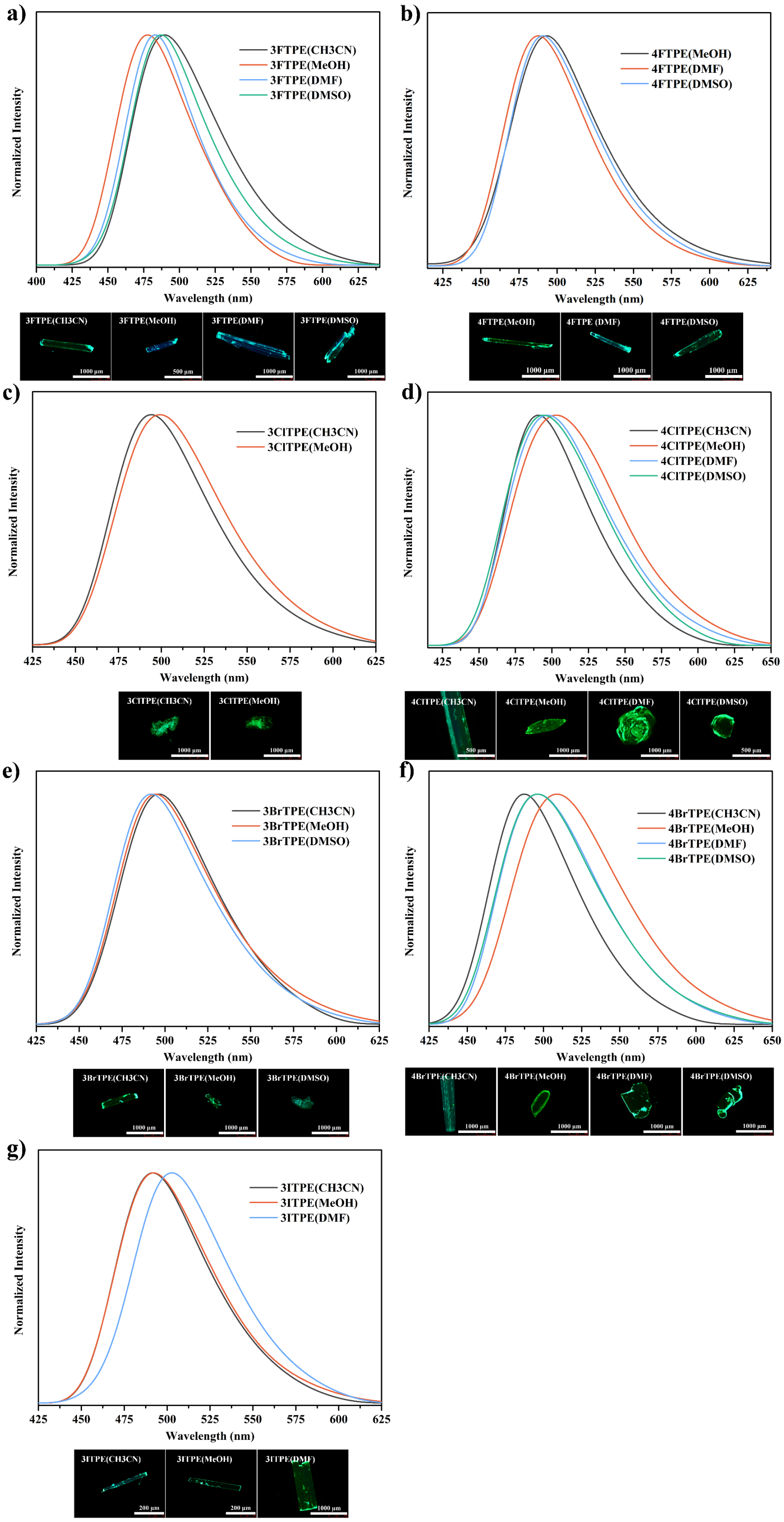

Figure S3. Fluorescence emission spectra and fluorescent images of **TPE** derivative crystals (λ_{ex} = 370 nm).

Table S1. Dihedral angle (θ) between **TPE** donor benzene ring and phenyl acetonitrile benzene ring in crystals.

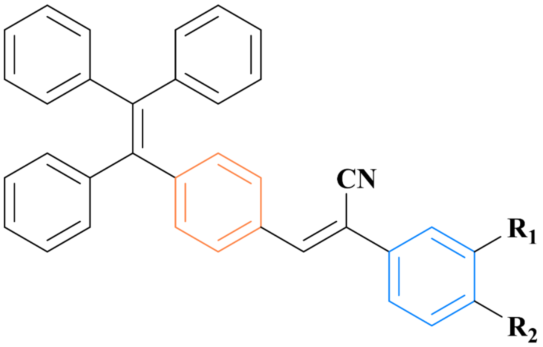

compounds	polymorphs	θ / °	conformation
3FTPE	Polymorph-1	7.57	coplanar
4FTPE	Polymorph-1	6.41, 6.42, 6.47, 6.55	coplanar
3ClTPE	Polymorph-1	5.16, 20.47	coplanar/twisted
4ClTPE	Polymorph-1	11.99	coplanar/twisted
	Polymorph-2	48.38, 52.95	
3BrTPE	Polymorph-1	7.51	coplanar/twisted
	Polymorph-2	33.71	
4BrTPE	Polymorph-1	14.33	coplanar/twisted
	Polymorph-2	47.70, 51.75	
3ITPE	Polymorph-1	8.78	coplanar

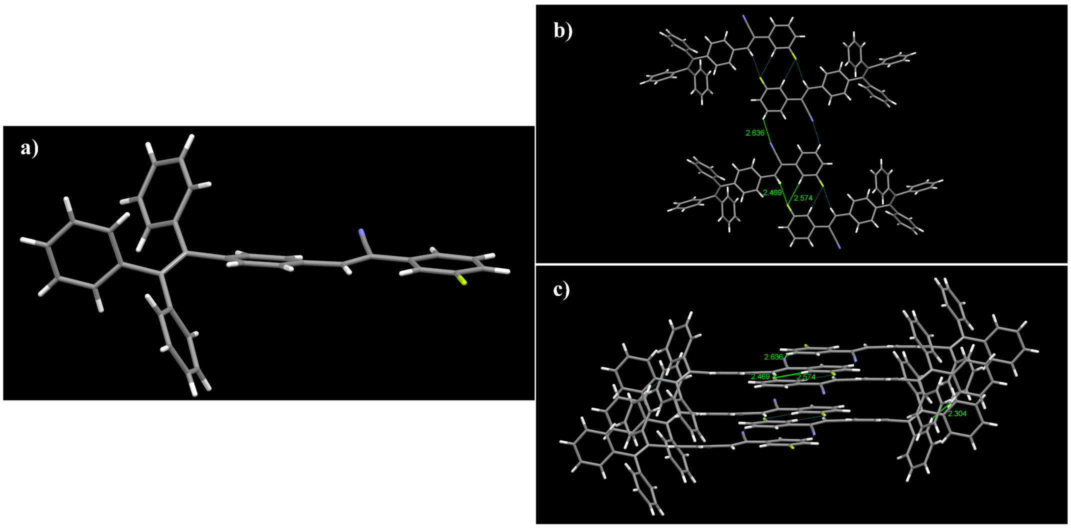

Figure S4. Molecular conformation (a), connection of dimers (b) and molecular packing (c) in the crystal lattice of **3FTPE**. Weak interactions were shown by blue dotted lines. C (grey), H (white), N (blue purple) and F (yellow). The $d_{\text{D-A}}$ distances are marked (Å).

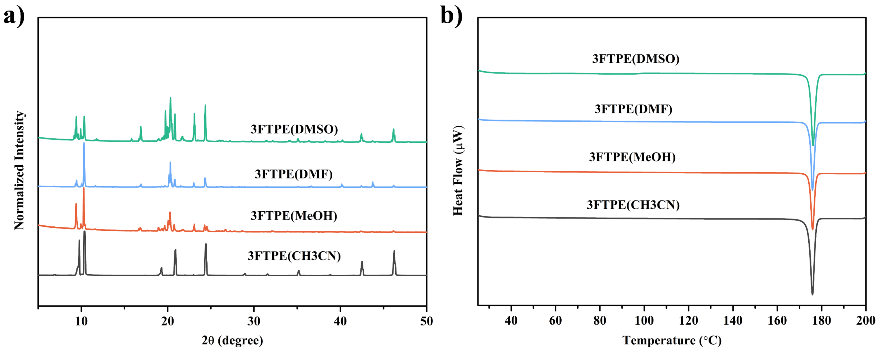

Figure S5. PXRD (a) and DSC (b) analysis of **3FTPE** crystals.

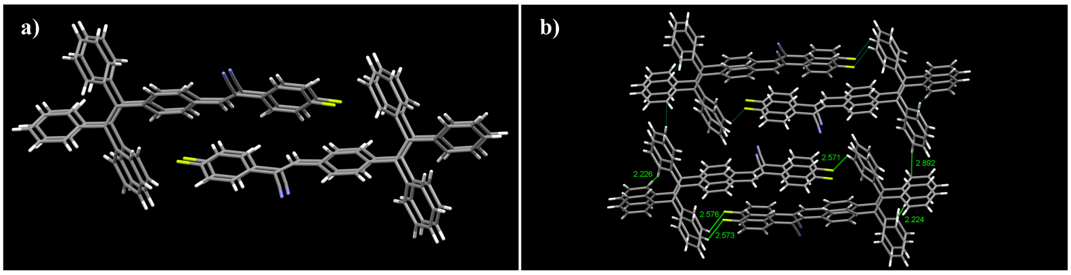

Figure S6. Molecular conformation (a) and molecular packing (b) in the crystal lattice of **4FTPE**. Weak interactions were shown by blue dotted lines. C (grey), H (white), N (blue purple) and F (yellow). The $d_{\text{D-A}}$ distances are marked (Å).

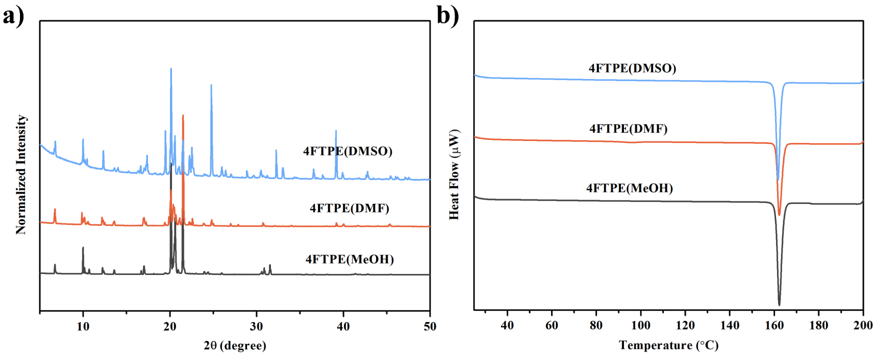

Figure S7. PXRD (a) and DSC (b) analysis of **4FTPE** crystals.

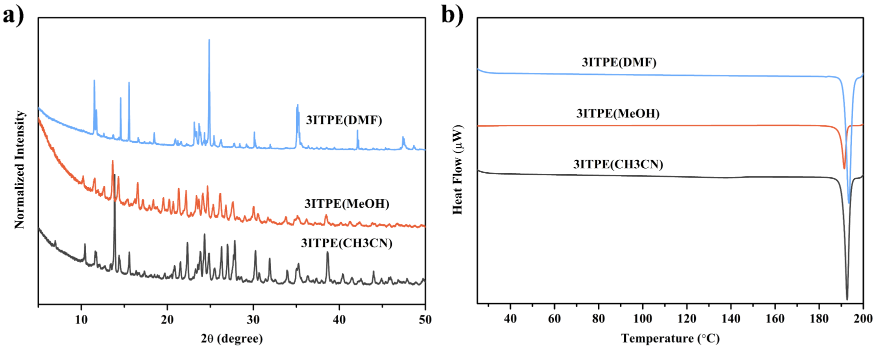

Figure S8. PXRD (a) and DSC (b) analysis of **3ITPE** crystals.

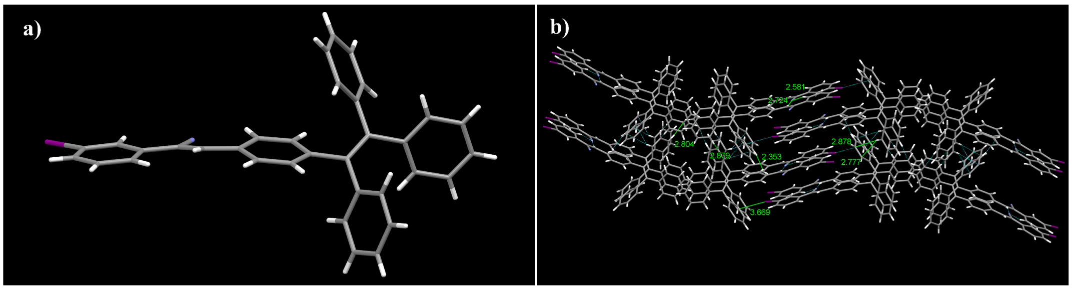

Figure S9. Molecular conformation (a) and molecular packing (b) in the crystal lattice of **3ITPE**. Weak interactions were shown by blue dotted lines. C (grey), H (white), N (blue purple) and I (purple red). The $d_{\text{D-A}}$ distances are marked (Å).

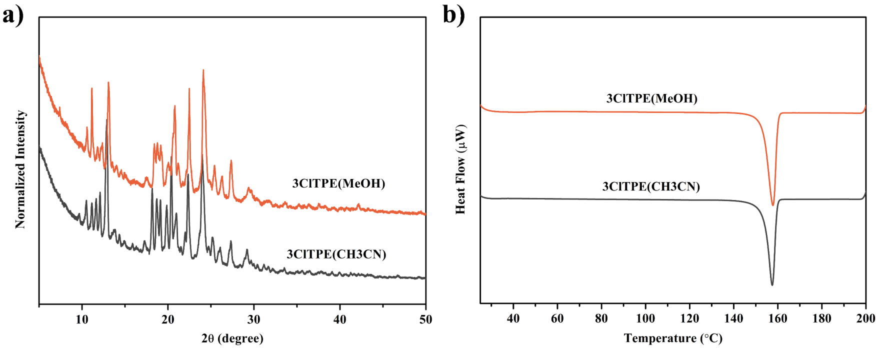

Figure S10. PXRD (a) and DSC (b) analysis of **3ClTPE** crystals.

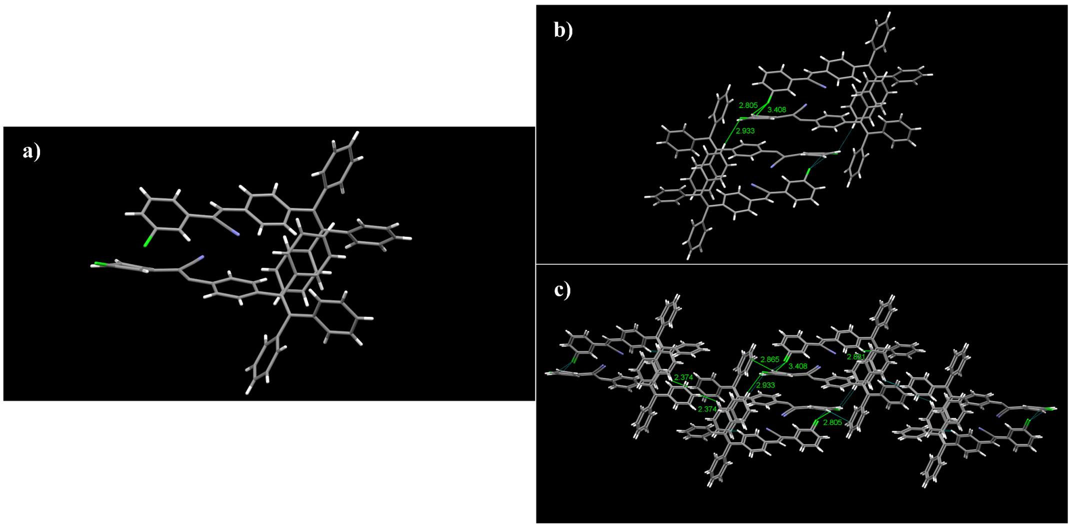

Figure S11. Molecular conformation (a), connection of asymmetric units (b) and molecular packing (c) in the crystal lattice of **3ClTPE**. Weak interactions were shown by blue dotted lines. C (grey), H (white), N (blue purple) and Cl (green). The $d_{\text{D-A}}$ distances are marked (Å).

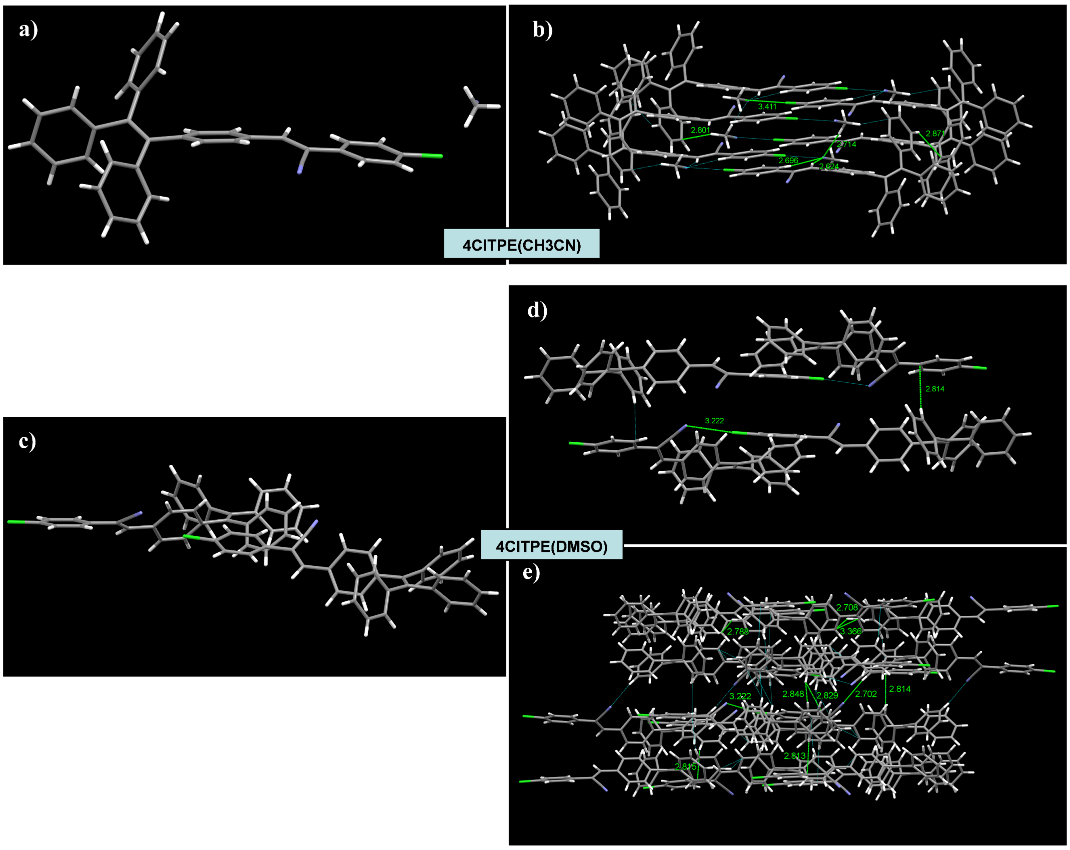

Figure S12. Molecular conformation (a, c), connection of asymmetric units (d) and molecular packing (b, e) in the crystal lattice of **4ClTPE**. Weak interactions were shown by blue dotted lines. C (grey), H (white), N (blue purple) and Cl (green). The $d_{D\text{-}A}$ distances are marked (Å).

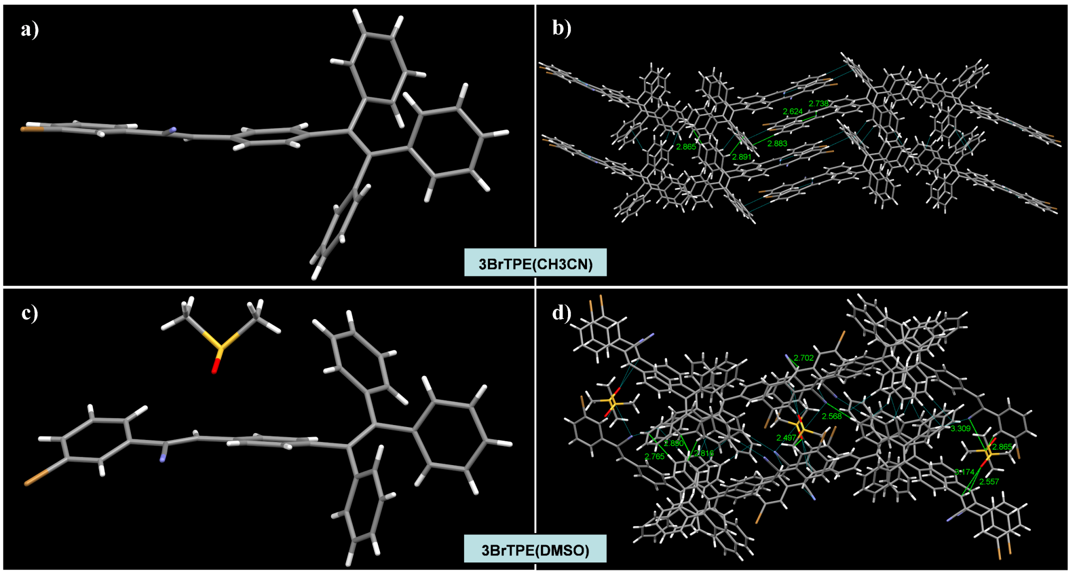

Figure S13. Molecular conformation (a, c) and molecular packing (b, d) in the crystal lattice of **3BrTPE**. Weak interactions were shown by blue dotted lines. C (grey), H (white), N (blue purple), S (yellow), O (red) and Br (brown). The $d_{D\text{-}A}$ distances are marked (Å).

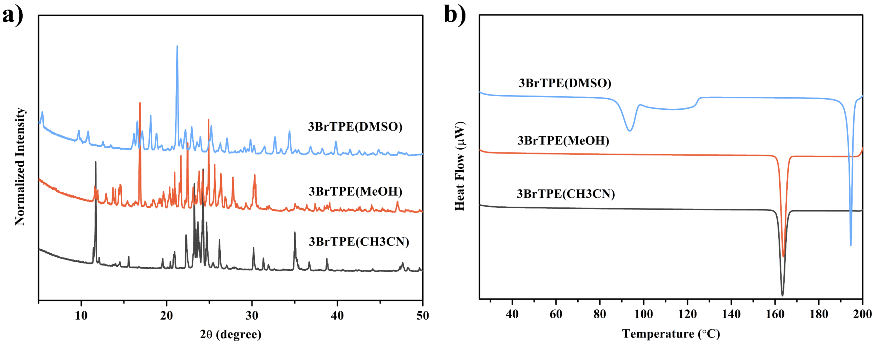

Figure S14. PXRD (a) and DSC (b) analysis of **3BrTPE** crystals.

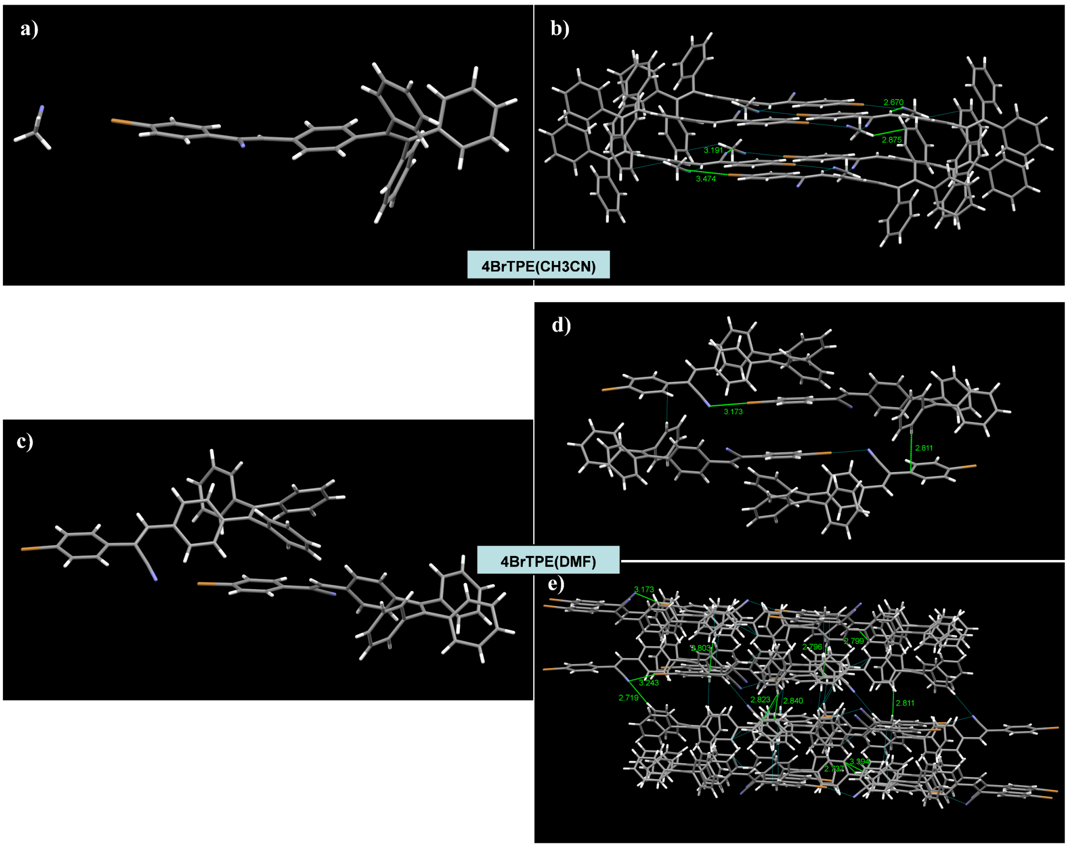

Figure S15. Molecular conformation (a, c), connection of asymmetric units (d) and molecular packing (b, e) in the crystal lattice of **4BrTPE**. Weak interactions were shown by blue dotted lines. C (grey), H (white), N (blue purple) and Br (brown). The $d_{\text{D-A}}$ distances are marked (Å).

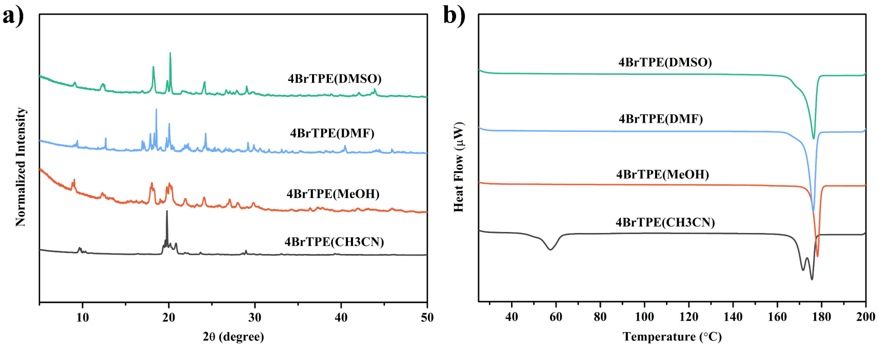

Figure S16. PXRD (a) and DSC (b) analysis of **4BrTPE** crystals.

5. Single-crystal to single-crystal transformation studies

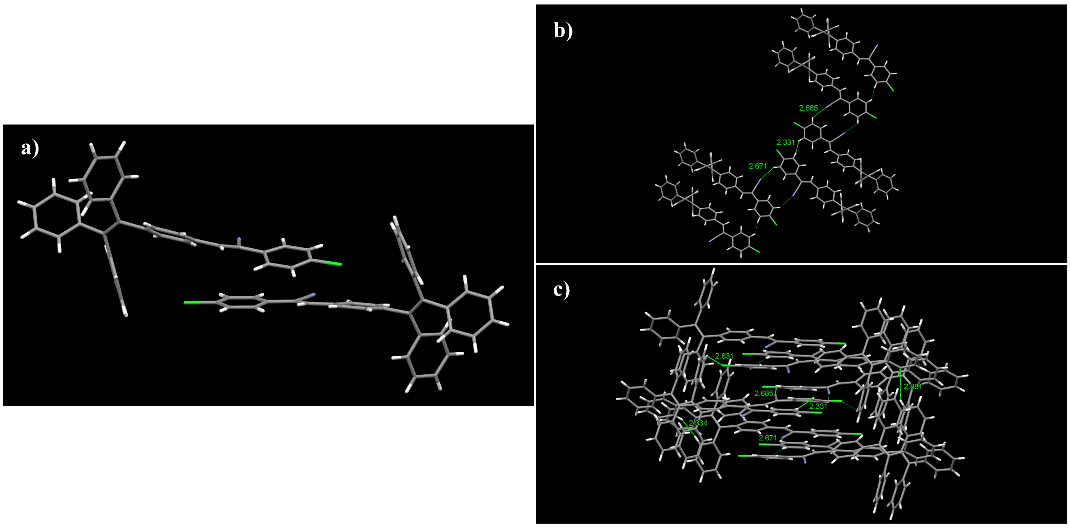

Figure S17. Molecular conformation (a), connection of dimers (b) and molecular packing (c) in the crystal lattice of **4ClTPE** (CH_3CN)(heated). Weak interactions were shown by blue dotted lines. C (grey), H (white), N (blue purple) and Cl (green). The $d_{D\text{-}A}$ distances are marked (Å).

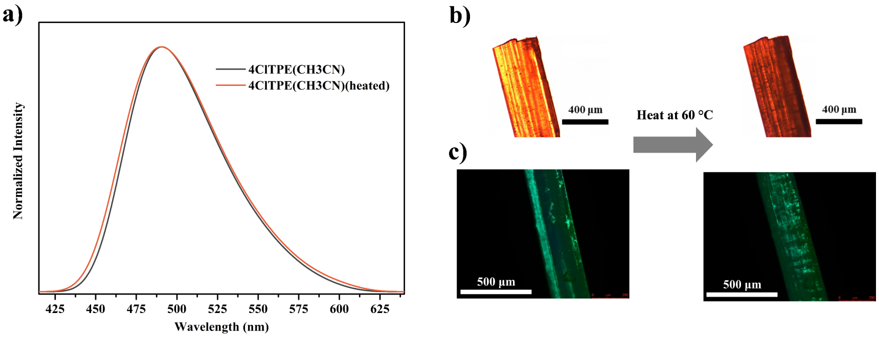

Figure S18. Fluorescence emission spectra (λ_{ex} = 370 nm) (a), fluorescence images (c) and images under a polarizing microscope (b) of **4ClTPE** (CH_3CN) crystal before and after heating.

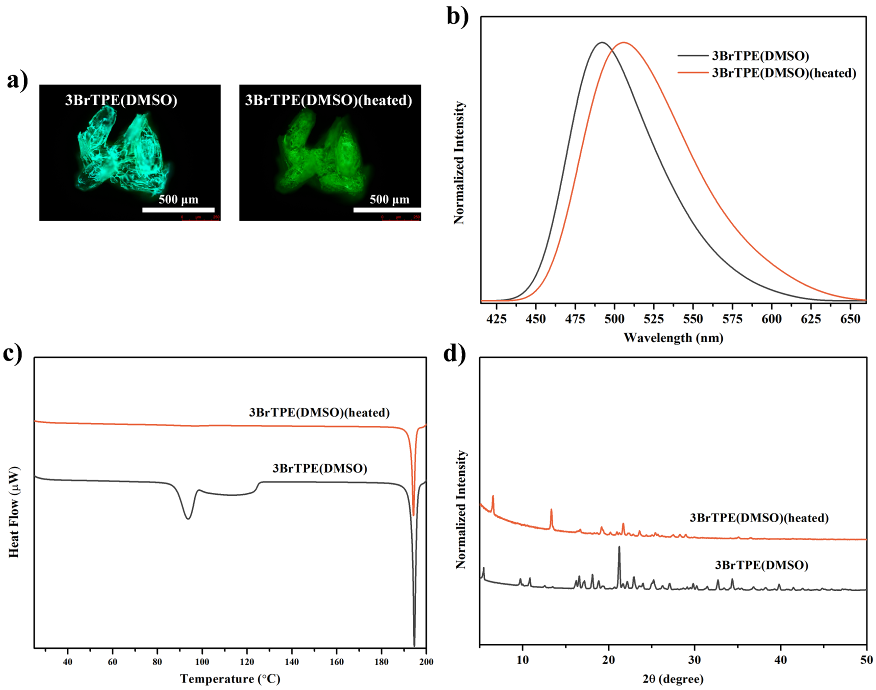

Figure S19. Fluorescent images (a), fluorescence emission spectra (λ_{ex} = 370 nm) (b), DSC analysis (c) and PXRD analysis (d) of **3BrTPE** (DMSO) crystal before and after heating.

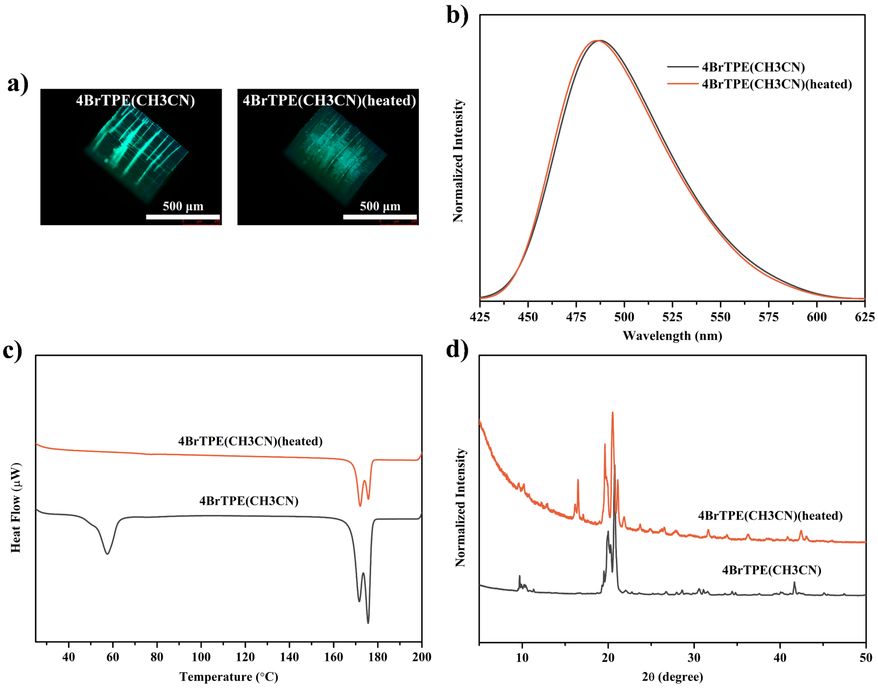

Figure S20. Fluorescent images (a), fluorescence emission spectra (λ_{ex} = 370 nm) (b), DSC analysis (c) and PXRD analysis (d) of **4BrTPE** (CH_3CN) crystal before and after heating.

6. Mechanofluorochromism studies

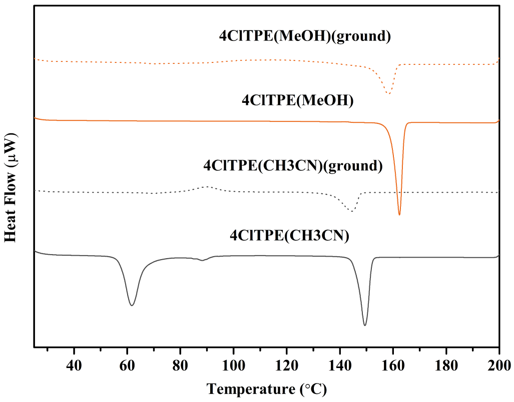

Figure S21. DSC analysis of **4ClTPE** crystal before and after grinding.

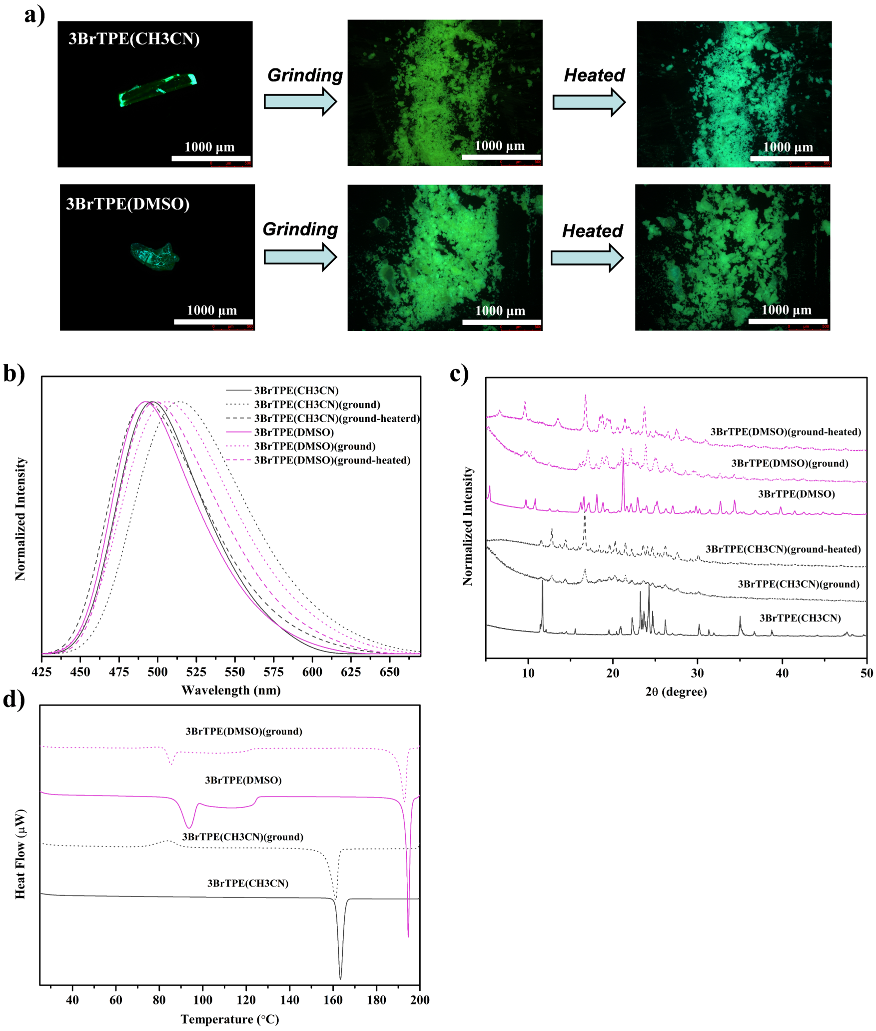

Figure S22. Mechanofluorochromism of **3BrTPE** crystals. Fluorescent images (a), fluorescence emission spectra (λ_{ex} = 370 nm) (b), PXRD analysis (c) and DSC analysis (d).

7. NMR and mass spectra of the compounds

7.1. ^{1}H and ^{13}C NMR spectra

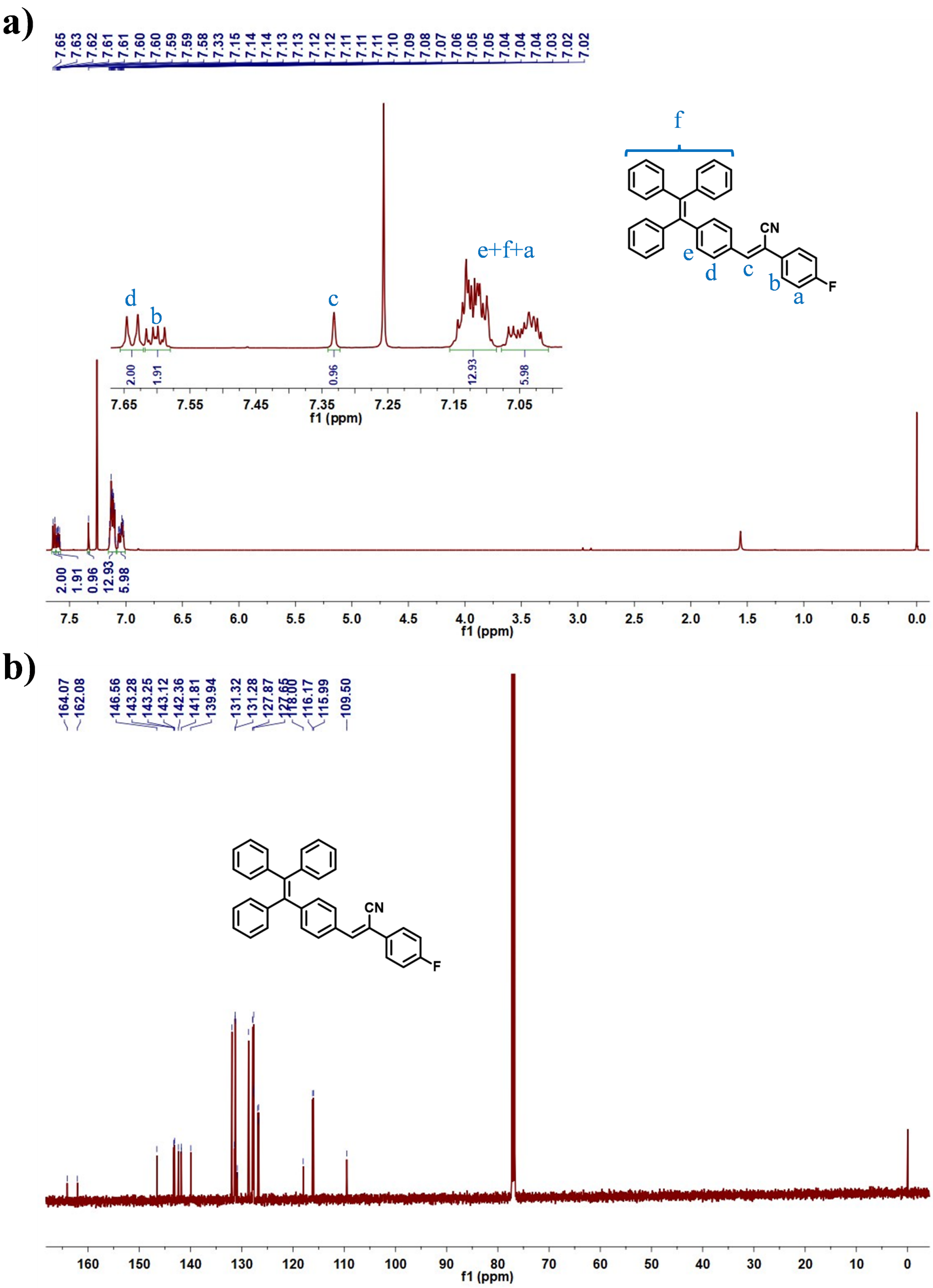

Figure S23. ^{1}H (a) and ^{13}C (b) NMR spectra of **4FTPE** in $CDCl_3$.

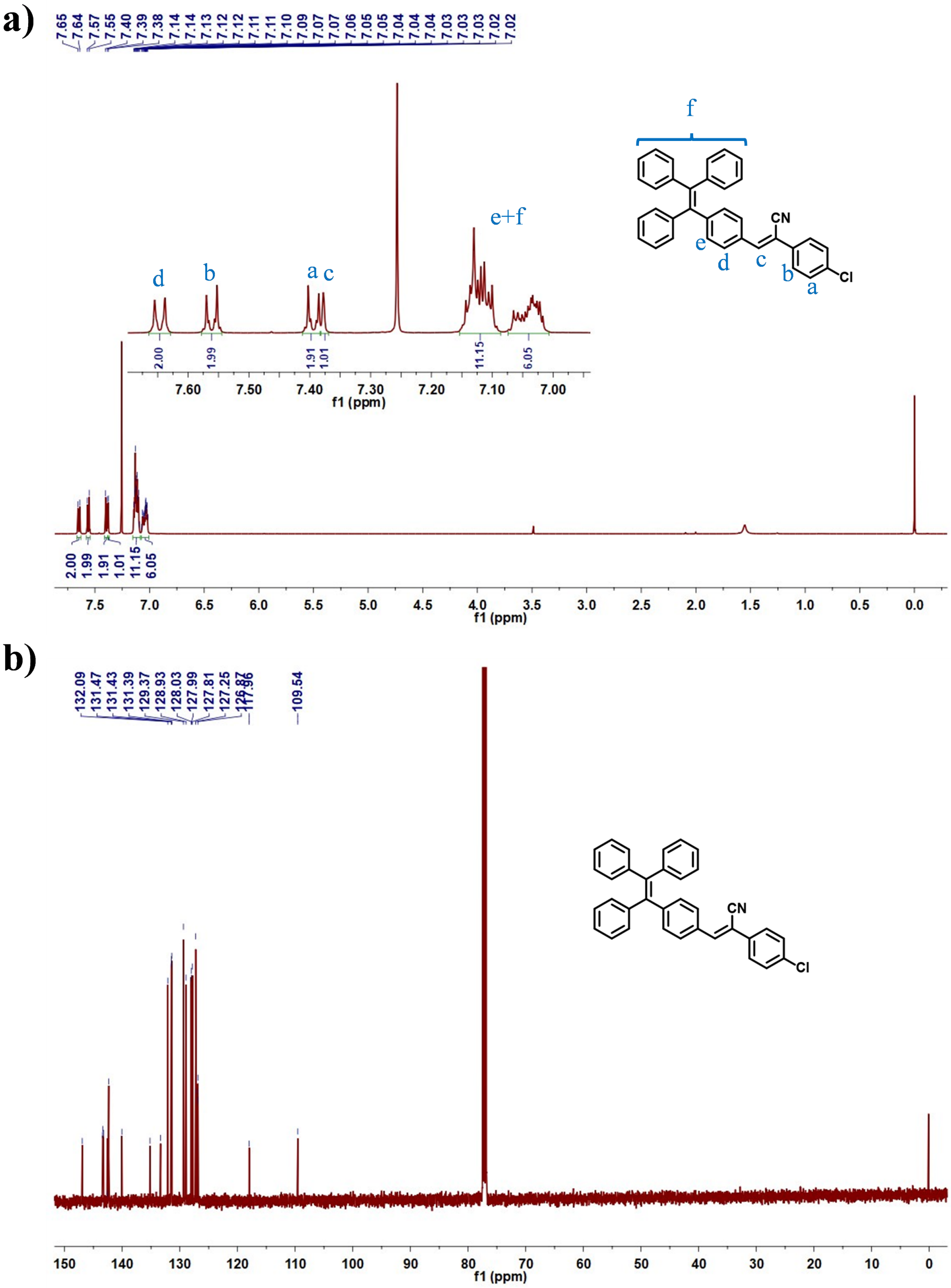

Figure S24. ^{1}H (a) and ^{13}C (b) NMR spectra of **4ClTPE** in $CDCl_3$.

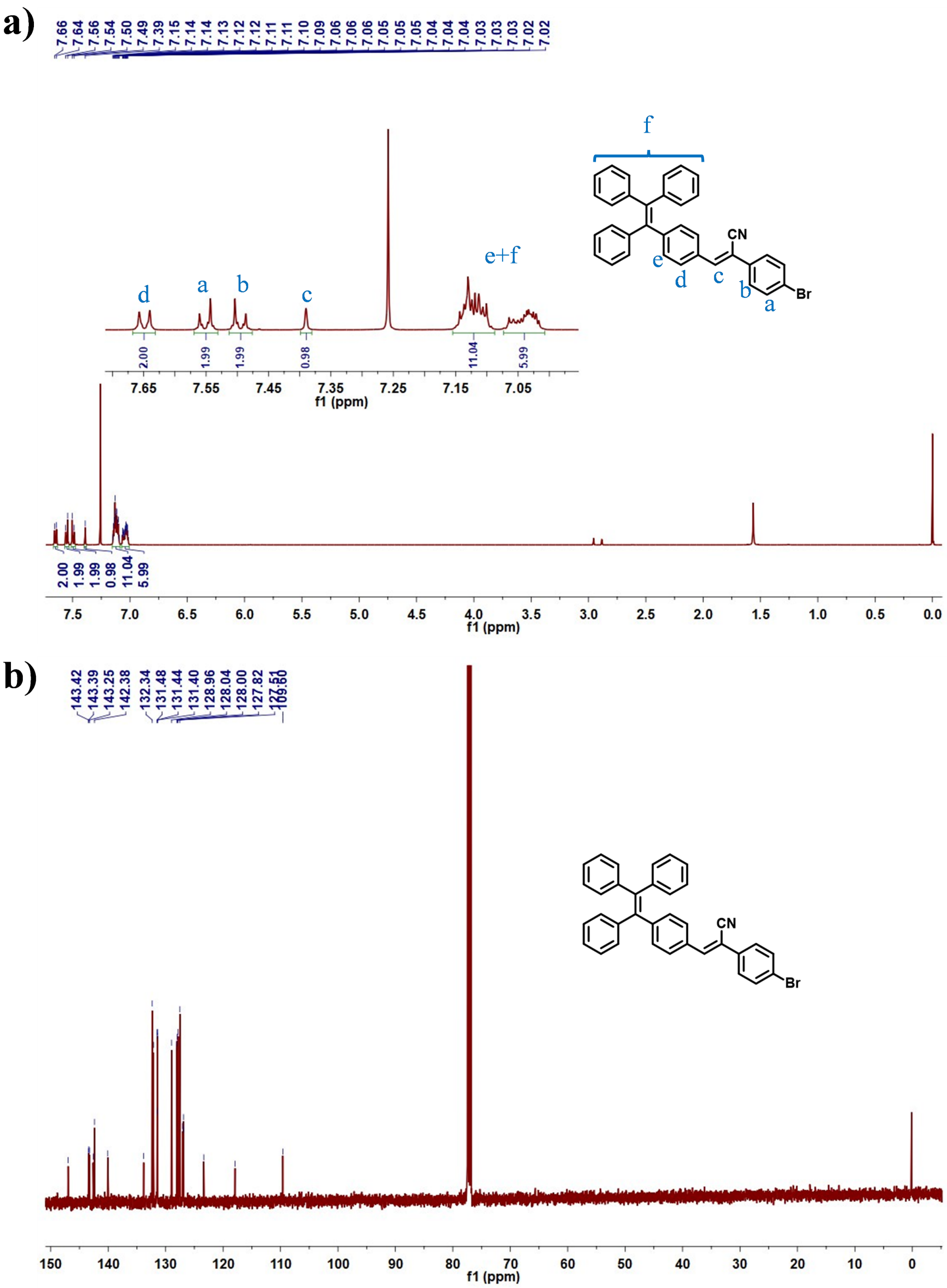

Figure S25. ^{1}H (a) and ^{13}C (b) NMR spectra of **4BrTPE** in $CDCl_3$.

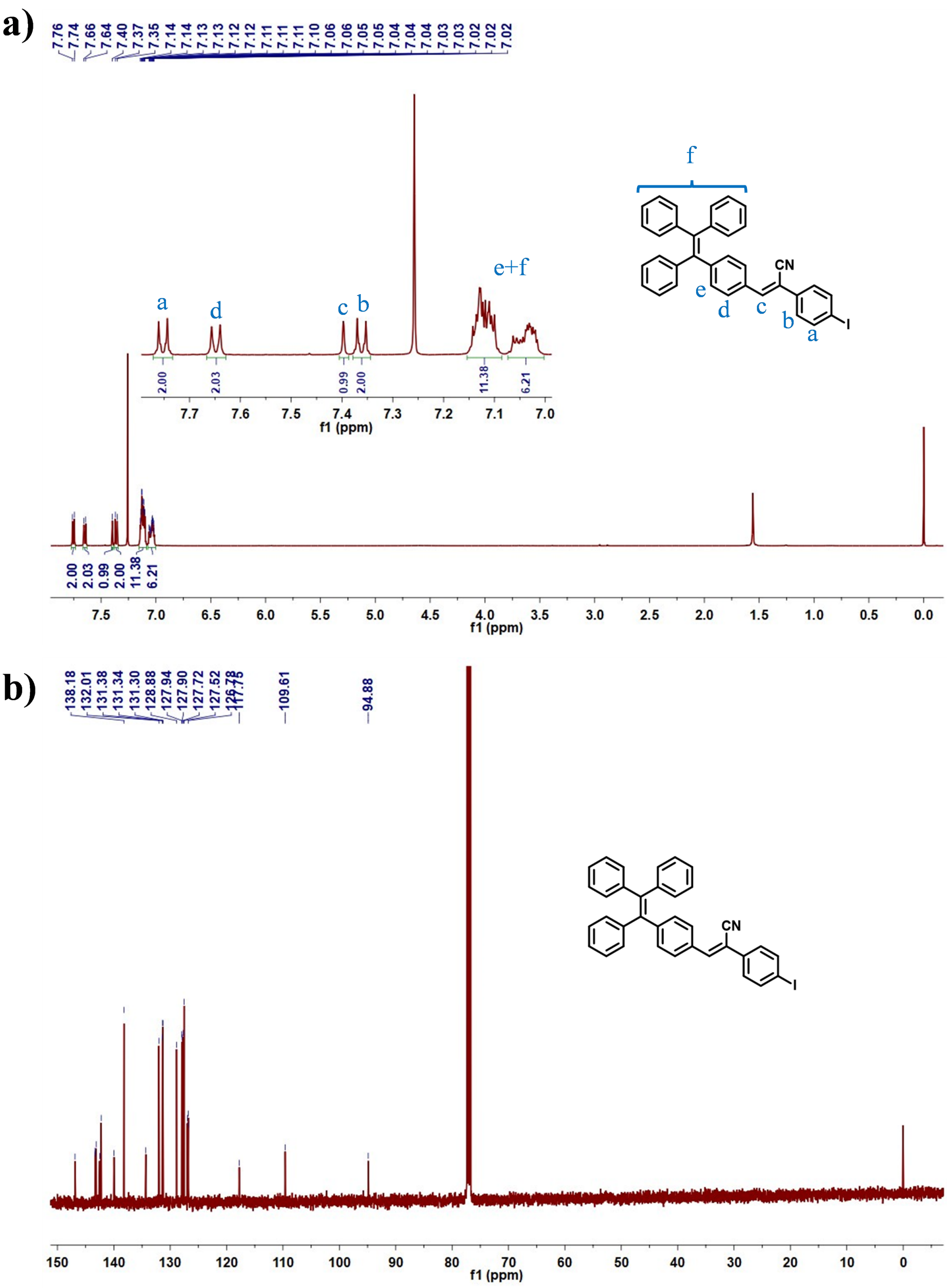

Figure S26. ^1H (a) and ^{13}C (b) NMR spectra of **4ITPE** in $CDCl_3$.

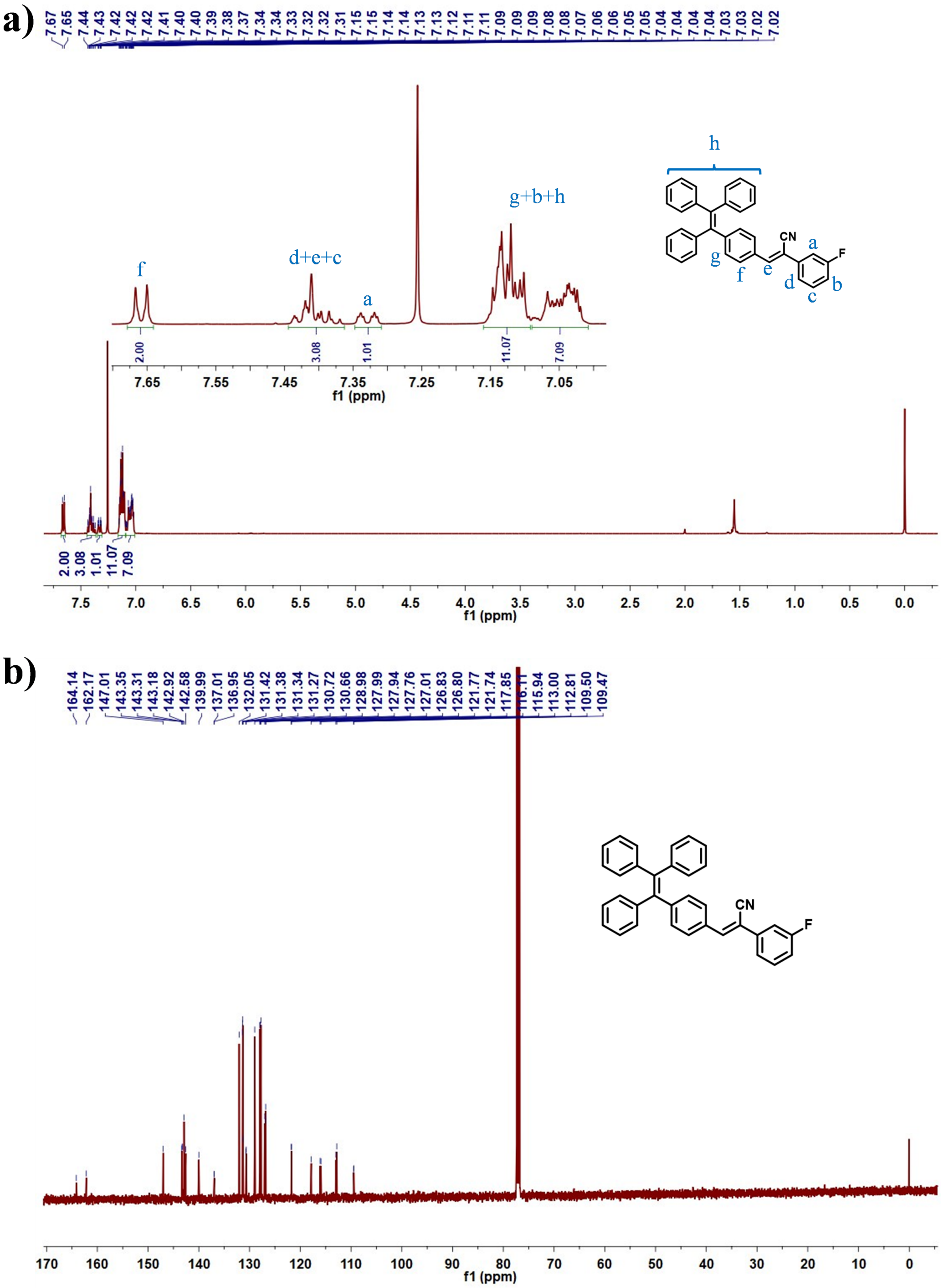

Figure S27. ^{1}H (a) and ^{13}C (b) NMR spectra of **3FTPE** in $CDCl_3$.

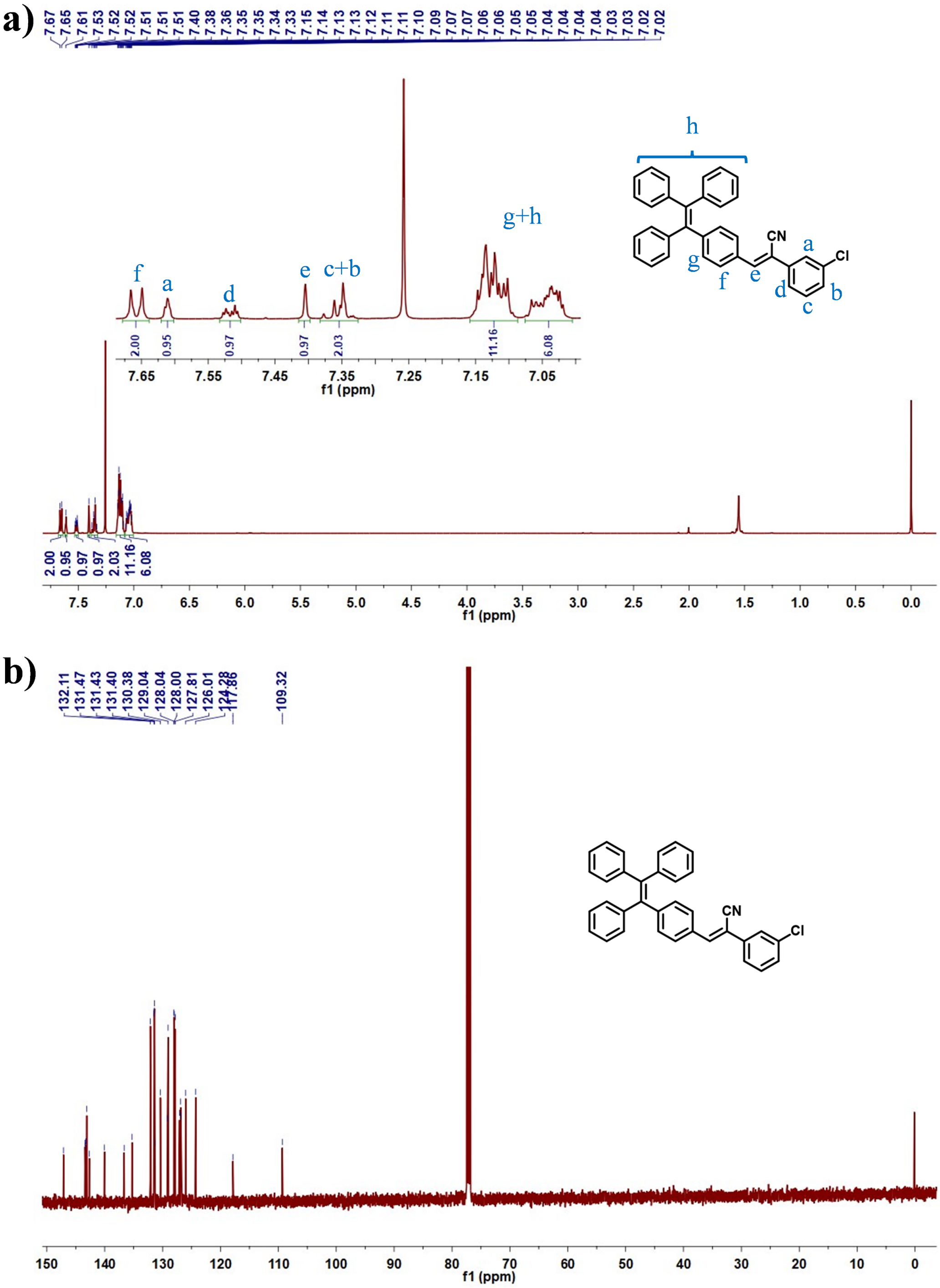

Figure S28. ^{1}H (a) and ^{13}C (b) NMR spectra of **3ClTPE** in $CDCl_3$.

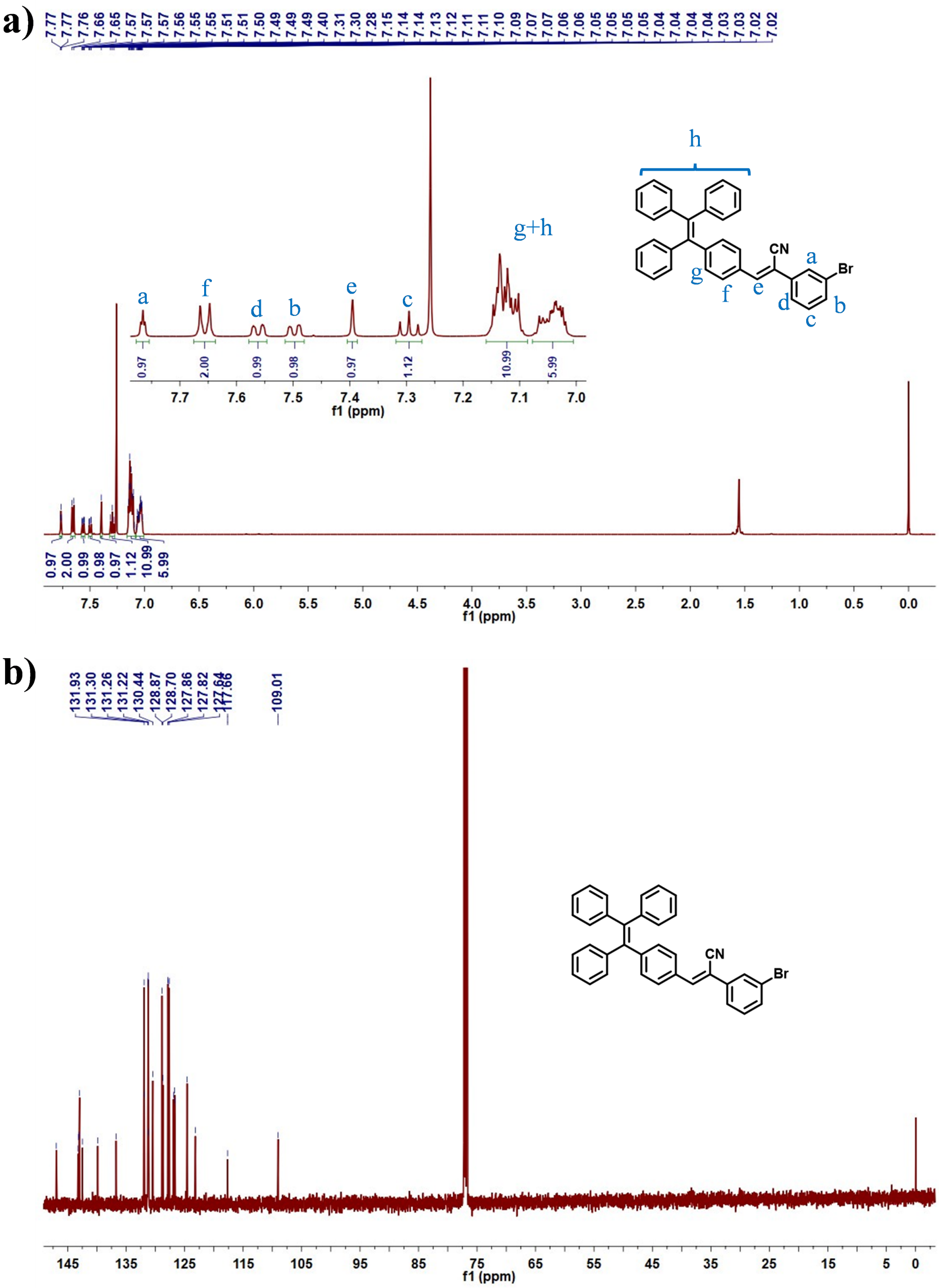

Figure S29. ^{1}H (a) and ^{13}C (b) NMR spectra of **3BrTPE** in $CDCl_3$.

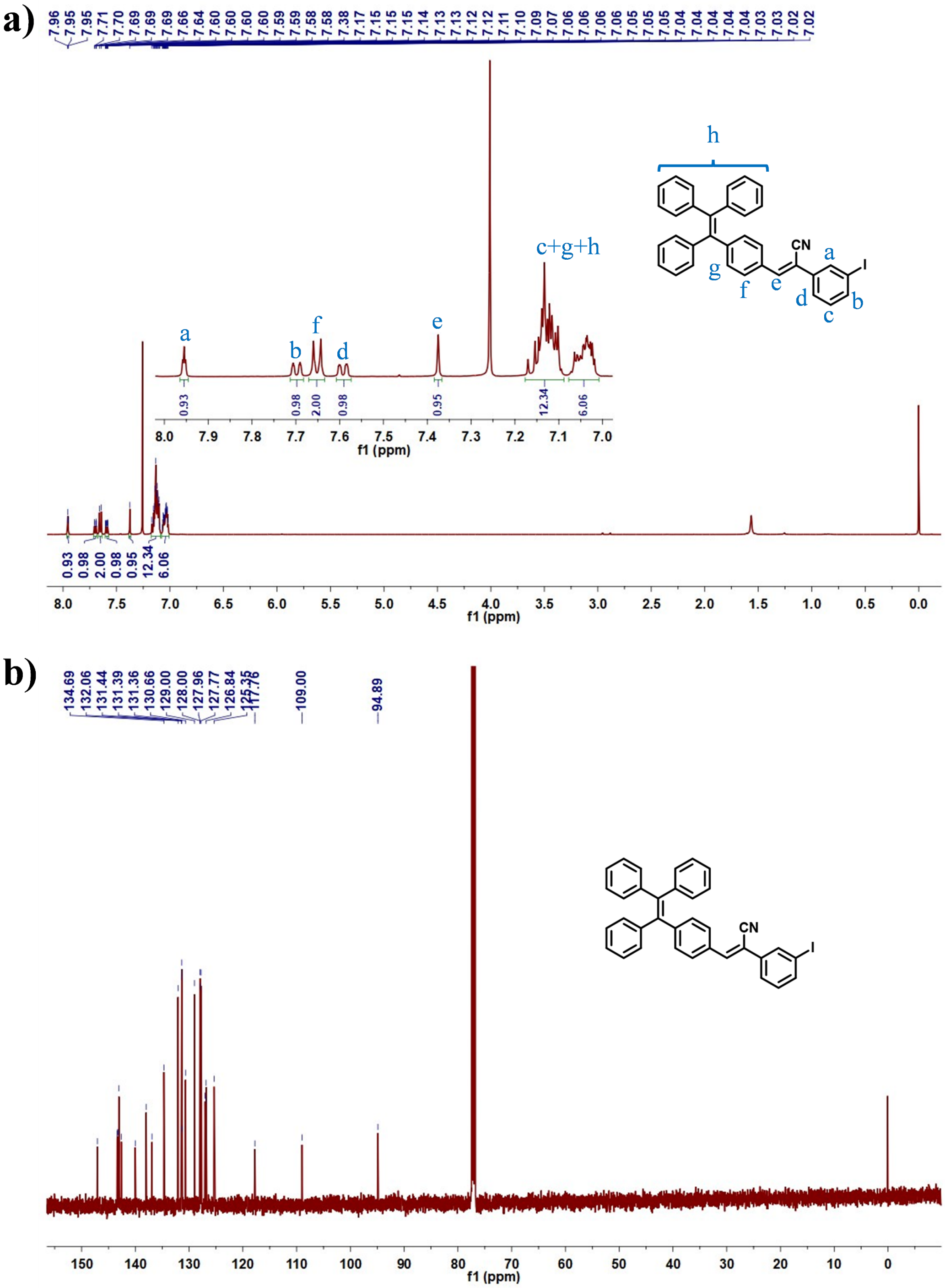

Figure S30. ^{1}H (a) and ^{13}C (b) NMR spectra of **3ITPE** in $CDCl_3$.

7.2. Mass spectra

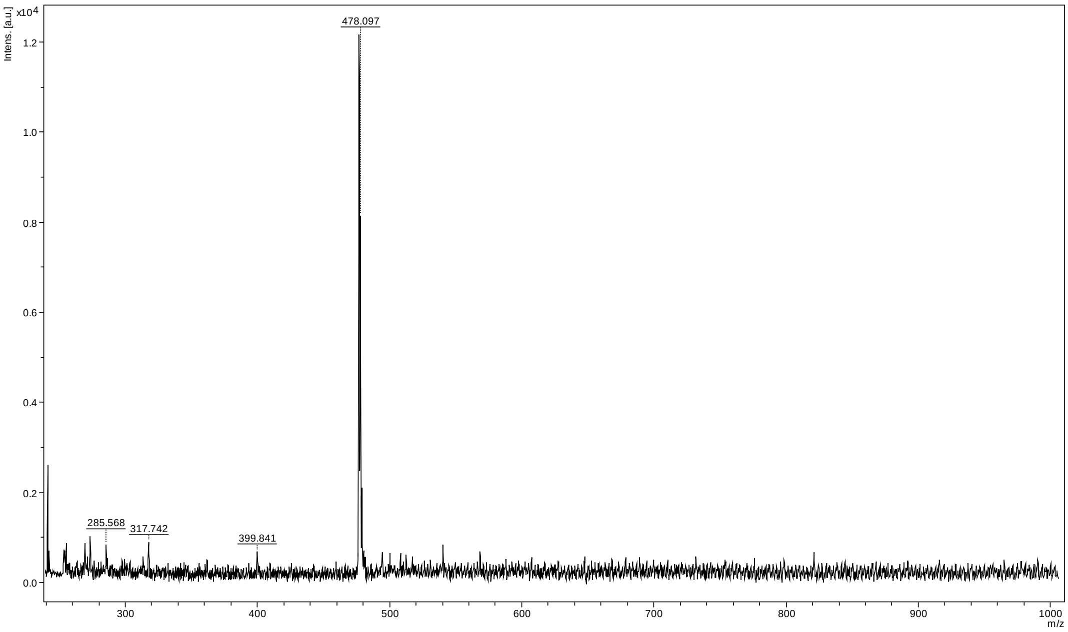

Figure S31. MALDI-TOF mass spectrum of **4FTPE**.

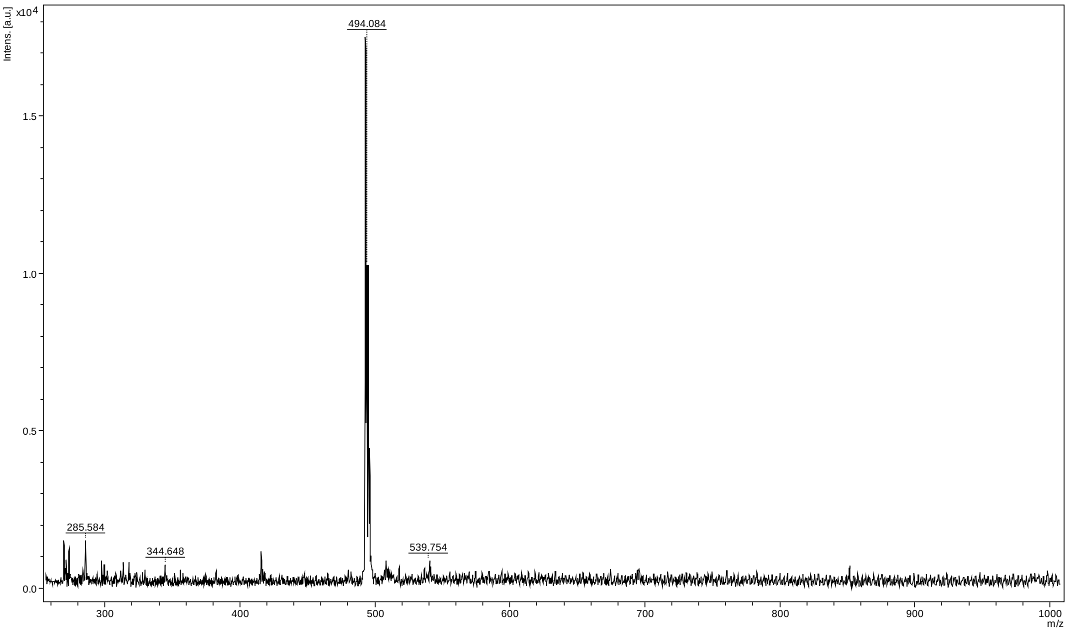

Figure S32. MALDI-TOF mass spectrum of **4ClTPE**.

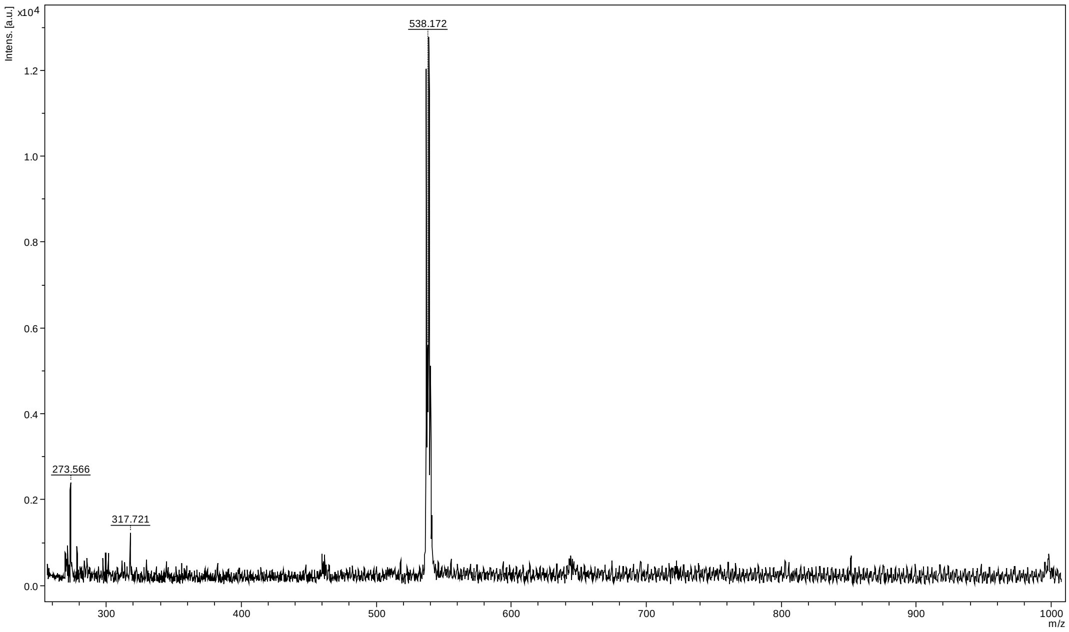

Figure S33. MALDI-TOF mass spectrum of **4BrTPE**.

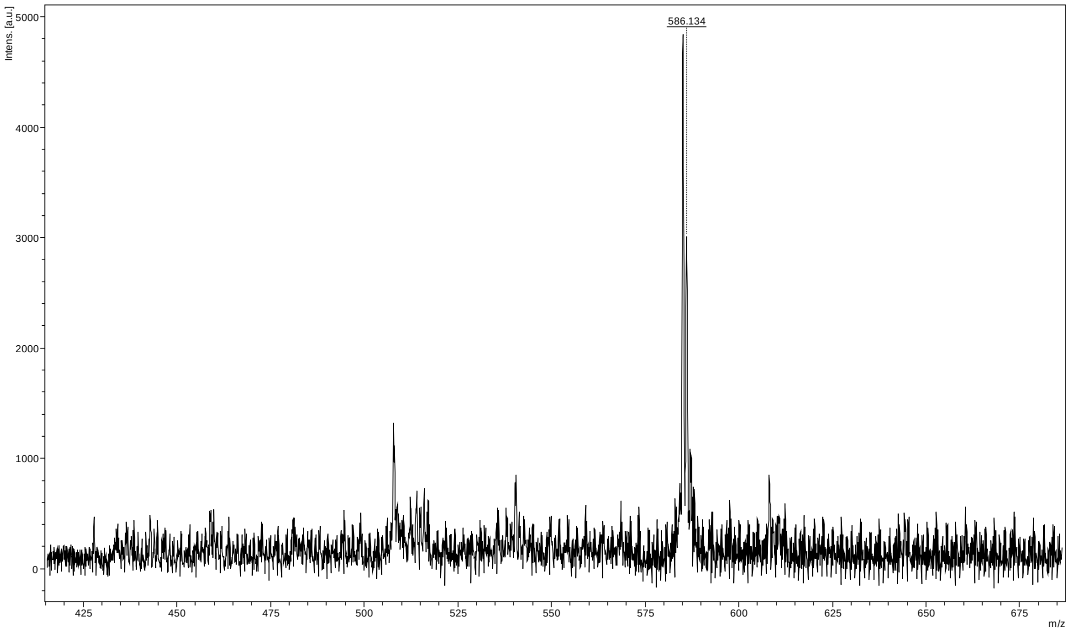

Figure S34. MALDI-TOF mass spectrum of **4ITPE**.

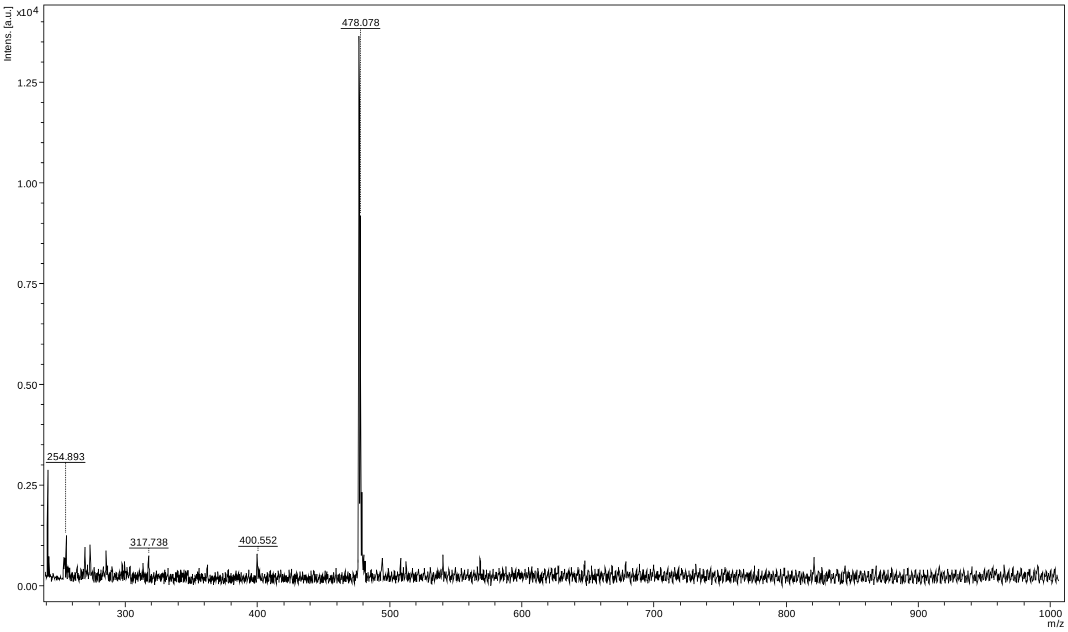

Figure S35. MALDI-TOF mass spectrum of **3FTPE**.

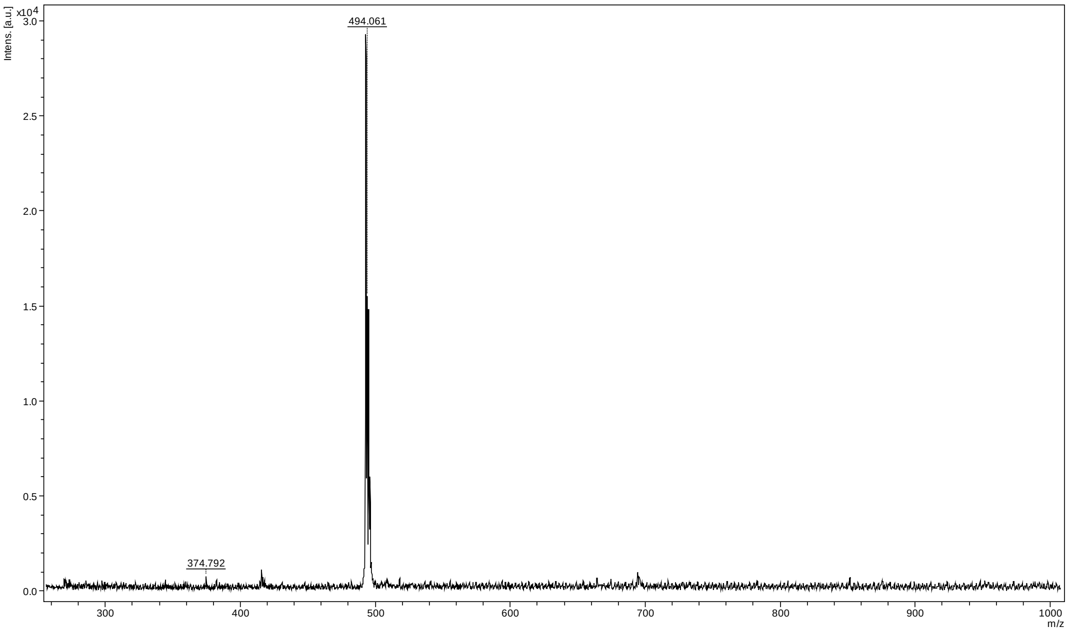

Figure S36. MALDI-TOF mass spectrum of **3ClTPE**.

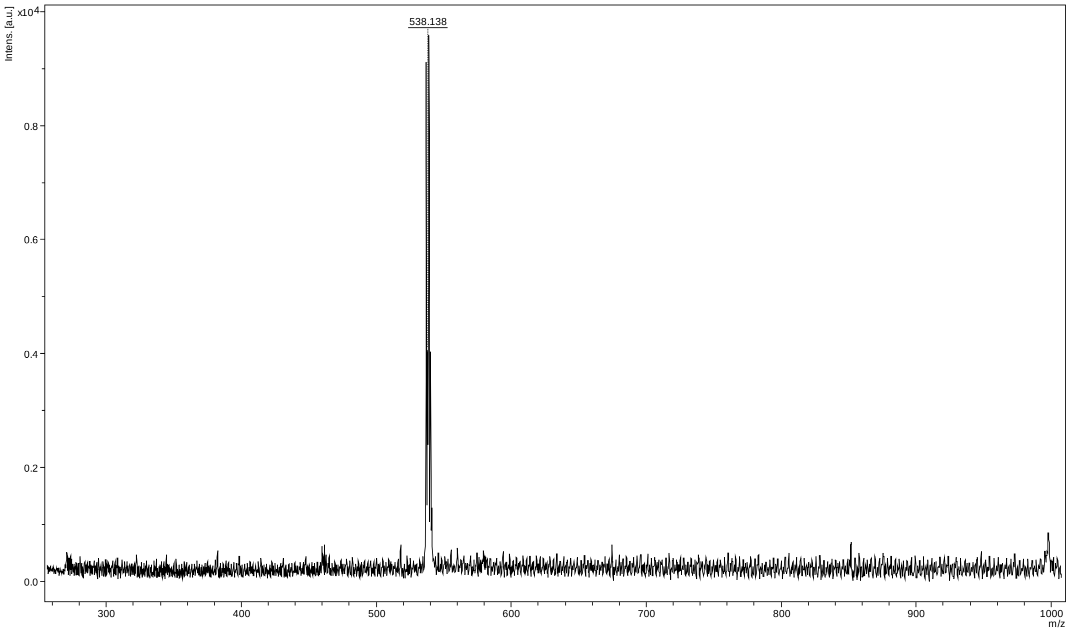

Figure S37. MALDI-TOF mass spectrum of **3BrTPE**.

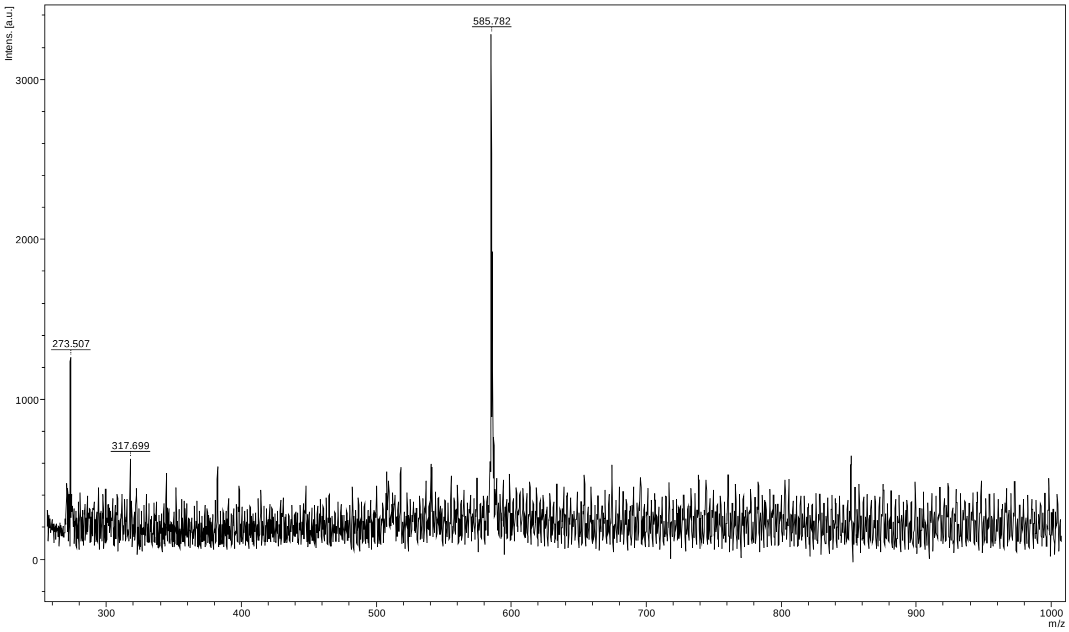

Figure S38. MALDI-TOF mass spectrum of **3ITPE**.

8. References

S1. Zhang, Yujian, et al. "Multicolored-fluorescence switching of ICT-type organic solids with clear color difference: mechanically controlled excited state." *Chemistry-A European Journal* 21.6 (2015): 2474-2479.